Gold(I)−Gold(III) Interactions in Polynuclear Sulfur-Centered Complexes. Synthesis and Structural Characterization of [S(Au$_2$dppf){Au(C$_6$F$_5$)$_3$}] and [{S(Au$_2$dppf)}$_2${Au(C$_6$F$_5$)$_2$}]OTf (dppf = 1,1′-Bis(diphenylphosphino)ferrocene)

Maria José Calhorda,[†] Fernando Canales,[‡] M. Concepción Gimeno,[‡] Josefina Jiménez,[‡] Peter G. Jones,[§] Antonio Laguna,*[,‡] and Luis F. Veiros[||]

ITQB, R. da Quinta Grande, 6, Aprt. 127, 2780 Oeiras, Portugal, Faculdade de Ciências, Ed. C1, 1700 Lisboa, Portugal, Departamento de Química Inorgánica, Instituto de Ciencia de Materiales de Aragón, Universidad de Zaragoza-CSIC, 50009 Zaragoza, Spain, Institut für Anorganische und Analytische Chemie der Technischen Universität, Postfach 3329, D-38023 Braunschweig, Germany, and Centro de Química Estrutural, Instituto Superior Técnico, 1096 Lisboa Codex, Portugal

Received February 14, 1997[⊗]

The reactions of [S(Au$_2$dppf)] (dppf = 1,1′-bis(diphenylphosphino)ferrocene) with the gold(III) precursors [Au(C$_6$F$_5$)$_3$(OEt$_2$)] and [Au(C$_6$F$_5$)$_2$(OEt$_2$)$_2$]OTf afford the mixed-valence complexes [S(Au$_2$dppf){Au(C$_6$F$_5$)$_3$}] (**1**) and [{S(Au$_2$dppf)}$_2${Au(C$_6$F$_5$)$_2$}]OTf (**2**). The crystal structures of these derivatives have been determined and show short gold(I)−gold(III) contacts of 3.404(1) Å in **1** and 3.2195(8) and 3.3661(10) Å in **2**. DFT calculations, including correlation and relativistic corrections, show that in these compounds where sulfur bridges three gold atoms it prefers to become pyramidal rather than planar, and Au(I)−Au(III) distances are indicative of a possible weak interaction. EH calculations suggest that such interaction is similar in origin to the well-studied Au(I)−Au(I) weak interactions and that it may occur in some real compounds.

Introduction

A strongly attractive and energetically favorable interaction has been observed between gold(I) atoms with d^{10} configurations in numerous polynuclear gold compounds.[1−5] It is manifested in molecular conformations with relatively close Au···Au interactions of *ca.* 3 Å, whose strength has been estimated with bond energies of ca. 33 kJ/mol.[6−9] This energy is comparable with that of standard hydrogen bonds and thus has similar consequences for the supramolecular chemistry of gold compounds. Intramolecular gold−gold contacts lend significant stabilization to multinuclear gold complexes, including in particular polynuclear heteroatom-centered cations.[1,2] The term aurophilicity has been coined for this phenomenon and has been the subject of a number of theoretical treatments, using advanced *ab initio* and density functional methods, including relativistic and correlation effects.[10−17] These studies have focused on gold(I) species, but in a polynuclear complex gold(I)−gold(III) interactions might also be possible. Our aim is to determine whether these contacts are present in gold compounds and to compare their strength with that of gold(I)−gold(I) interactions.

We are currently working on sulfur-centered phosphine−gold complexes, and we have previously reported the synthesis and structural characterization of the gold(I) tetraaurated species [S(AuPPh$_3$)$_4$]$^{2+}$ [18,19] and [S(Au$_2$dppf)$_2$(AuPPh$_2$Me)$_2$]$^{2+}$.[20] Furthermore, we have described the first examples of the synthesis and crystal structures of the novel μ_4-sulfido tetranuclear mixed gold(I)−gold(III) derivatives,[21] which show a tetrahedral geometry at the sulfur center, in contrast to the square-

[†] ITQB and Faculdade de Ciencias.
[‡] Universidad de Zaragoza-CSIC.
[§] Technische Universität Braunschweig.
[||] Instituto Superior Técnico.
[⊗] Abstract published in *Advance ACS Abstracts,* August 1, 1997.

(1) Schmidbaur, H. *Interdiscip. Sci. Rev.* **1992**, *17*, 213.
(2) Schmidbaur, H. *Pure Appl. Chem.* **1993**, *65*, 691.
(3) Yang, Y.; Ramamoorthy, V.; Sharp, P. R. *Inorg. Chem.* **1993**, *32*, 1946.
(4) Jones, P. G. *Gold Bull.* **1981**, *14*, 102; **1983**, *16*, 114; **1986**, *19*, 46.
(5) Schmidbaur, H. *Chem. Soc. Rev.* **1995**, 391.
(6) Dziwok, K.; Lachmann, J.; Wilkinson, D. L.; Müller, G.; Schmidbaur, H. *Chem. Ber.* **1990**, *123*, 423.
(7) Schmidbaur, H.; Dziwok, K.; Grohmann, A.; Müller, G. *Chem. Ber.* **1989**, *122*, 893.
(8) Schmidbaur, H.; Graf, W.; Müller, G. *Angew. Chem., Int. Ed. Engl.* **1988**, *27*, 417.
(9) Narayanaswamy, R.; Young, M. A.; Parkhurst, E.; Ouellette, M.; Kerr, M. E.; Ho, D. M.; Elder, R. C.; Bruce, A. E.; Bruce, M. R. M. *Inorg. Chem.* **1993**, *32*, 2506.
(10) Rösch, N.; Görling, A.; Ellis, D. E.; Schmidbaur, H. *Angew. Chem. Int. Ed. Engl.* **1989**, *28*, 1357.
(11) Pyykkö, P.; Zhao, Y. *Angew. Chem., Int. Ed. Engl.* **1991**, *30*, 604.
(12) Görling, A.; Rösch, N.; Ellis, D. E.; Schmidbaur, H. *Inorg. Chem.* **1991**, *30*, 3986.
(13) Li, J.; Pyykkö, P. *Inorg. Chem.* **1993**, *32*, 2630.
(14) Burdett, J. K.; Eisenstein, O.; Schweizer, W. B. *Inorg. Chem.* **1994**, *33*, 3261.
(15) Pyykkö, P.; Li, J. *Chem. Phys. Lett.* **1994**, *218*, 133.
(16) Häberlen, O. D.; Schmidbaur, H.; Rösch, N. *J. Am. Chem. Soc.* **1994**, *116*, 8241.
(17) Pyykkö, P.; Angermaier, K.; Assmann, B.; Schmidbaur, H. *J. Chem. Soc., Chem. Commun.* **1995**, 1889.
(18) Canales, F.; Gimeno, M. C.; Jones, P. G.; Laguna, A. *Angew. Chem., Int. Ed. Engl.* **1994**, 769.
(19) Canales, F.; Gimeno, M. C.; Laguna, A.; Villacampa, M. D. *Inorg. Chim. Acta* **1996**, *244*, 95.
(20) Canales, F.; Gimeno, M. C.; Laguna, A.; Jones, P. G. *J. Am. Chem. Soc.* **1996**, *118*, 4839.
(21) Canales, F.; Gimeno, M. C.; Laguna, A.; Jones, P. G. *Organometallics* **1996**, *15*, 3412.

S0276-7333(97)00114-3 CCC: $14.00

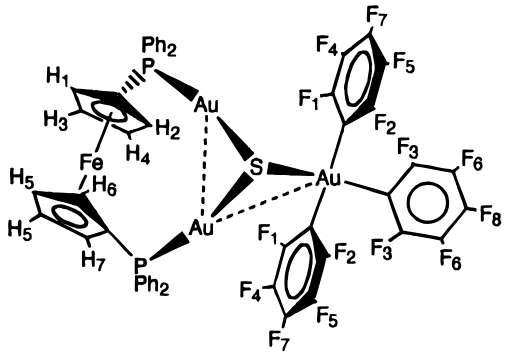

Figure 1. Numerical assignation of the protons and fluorine atoms for NMR spectra.

pyramidal structure in the above-mentioned gold(I) complexes. In one of the mixed-valence species a weak gold(I)−gold(III) contact was established by a crystal structure determination. Here we report further syntheses of mixed-valent sulfur-centered derivatives whose crystal structures have revealed gold(I)−gold(III) interactions only slightly longer than those reported for gold(I). Gold(I)−gold(III) interactions have been previously described in mixed-valence doubly bridged ylide systems where the gold atoms are forced to be in close proximity.[22−25]

Results and Discussion

Chemical Studies. The reaction of [S(Au_2dppf)] (dppf = 1,1′-bis(diphenylphosphino)ferrocene) with [Au(C_6F_5)$_3$(OEt_2)] (molar ratio 1:1) leads to the trinuclear mixed-valence species [S(Au_2dppf){Au(C_6F_5)$_3$}] (**1**). Complex **1** is an orange solid, moisture- and air-stable, and has conductivity values consistent with a neutral compound. Its IR spectrum shows bands at 1506 (vs) and 969 (vs) cm^{-1} arising from the pentafluorophenyl group bonded to a gold(III) center; the ν(Au−S) vibration appears at 315 (w) cm^{-1}.

The $^{31}P\{^1H\}$ NMR spectrum at room temperature shows a singlet at 28.4 ppm and a broad signal at 25.5 ppm; when the experiment is carried out at low temperature (−55 °C), two singlets appear at 27.7 and 27.1 ppm, which indicates the inequivalence of the phosphorus atoms of dppf. The ^1H NMR spectrum at room temperature shows two multiplets for the α- and β-protons of the cyclopendienyl rings, sharpening into seven multiplets at −55 °C. These multiplets correspond to the inequivalent protons of the Cp rings (see Figure 1 and Table 1). The ^{19}F NMR spectrum shows three multiplets for the *ortho* fluorine in the ratio 1:1:1, two triplets for the *para* fluorine with a 2:1 ratio, and two multiplets for the *meta* fluorine in the ratio 2:1. The presence of two triplets for the *para* fluorine indicates the presence of an Au(C_6F_5)$_3$ group where the two mutually *trans* pentafluorophenyl units are equivalent; however, this should imply only two multiplets in a 2:1 ratio for the *ortho* and *meta* fluorines, whereas the *ortho* fluorines show three multiplets. The reason could be that the normal rotation of the pentafluorophenyl rings, which renders these positions equivalent, cannot take place for the mutually *trans* C_6F_5 rings; then three multiplets should appear for the *ortho* and *meta* fluorines in a 1:1:1 ratio. This is observed for the *ortho* fluorine, but in the resonances of the *meta* fluorine two of the multiplets must be overlapped.

Table 1. NMR Data for Complex 1[a]

nucleus	δ, ppm
$^{31}P\{^1H\}$	27.7(s), 27.1 (s)
^1H	5.02 (m), 4.90 (m) (H_3, H_4)
	4.47 (m) (H_5)
	4.21 (m), 4.00 (m) (H_1, H_2)
	3.39 (m), 3.29 (m) (H_6, H_7)
^{19}F	−118.1 (m), −120.3 (m) (F_1, F_2)
	−122.4 (m) (F_3)
	−157.9 (t) (F_7), $^3J_{FF}$ = 20.67 Hz
	−158.8 (t) (F_8) $^3J_{FF}$ = 20.67 Hz
	−161.8 (m) (F_4 + F_5)
	−162.5 (m) (F_6)

[a] Measured in $CDCl_3$ at −55 °C: s = singlet, t = triplet, m = multiplet.

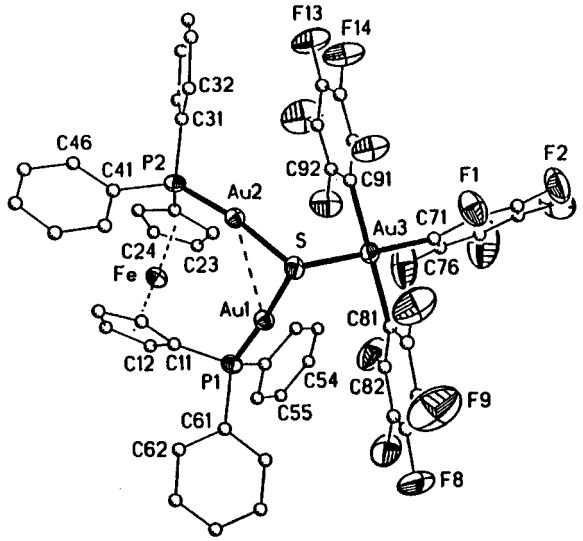

Figure 2. The structure of complex **1** in the crystal. Displacement parameter ellipsoids represent 50% probability surfaces. Carbon atoms are spheres of arbitrary radius. The H atoms are omitted for clarity.

In the positive-ion mass (FAB) spectrum of **1** the molecular peak does not appear, nor does any peak containing the unit Au(C_6F_5)$_3$. Under FAB conditions the formation of the thiolate $C_6F_5S^-$ is detected and also the presence of one fragment at m/z = 1147 assigned to $[Au_2(SC_6F_5)(dppf)]^+$.

The structure of complex **1** has been confirmed by an X-ray diffraction study. The molecule is shown in Figure 2, and a selection of bond lengths and angles are collected in Table 2. The geometry of the molecule is trigonal pyramidal at the sulfur atom, which lies 1.29 Å out of the plane of the three gold atoms. The three Au−Au distances in the molecule are very dissimilar. The distance between the two gold(I) atoms is the shortest, 2.8889(8) Å, whereas the two gold(I)−gold(III) distances are 3.404(1) and 3.759(1) Å. These data indicate the existence of an Au(I)···Au(III) interaction that, although weak, is able to reduce the symmetry in the molecule and thus render the gold(I) atoms inequivalent. This inequivalence is also detected in solution in the $^{31}P\{^1H\}$ NMR spectrum. The Au−S−

(22) Mazany, A. M.; Fackler, J. P., Jr. *J. Am. Chem. Soc.* **1984**, *106*, 801.
(23) Fackler, J. P., Jr.; Trzcinska-Bancroft, B. *Organometallics* **1985**, *4*, 1891.
(24) Raptis, R. G.; Porter, L. C.; Emrich, R. J.; Murray, H. H.; Fackler, J. P., Jr. *Inorg. Chem.* **1990**, *29*, 4408.
(25) Schmidbaur, H.; Hartmann, C.; Reber, G.; Müller, G. *Angew. Chem. Int. Ed. Engl.* **1987**, *26*, 1146.

Table 2. Selected Bond Lengths (Å) and Angles (deg) for Complex 1

Au(1)−P(1)	2.244(3)	Au(1)−S	2.332(3)
Au(1)−Au(2)	2.8889(8)	Au(2)−P(2)	2.245(4)
Au(2)−S	2.342(4)	Au(3)−C(71)	2.02(2)
Au(3)−C(81)	2.061(14)	Au(3)−C(91)	2.079(13)
Au(3)−S	2.374(4)	P(1)−C(11)	1.77(2)
P(1)−C(51)	1.80(2)	P(1)−C(61)	1.820(14)
P(2)−C(21)	1.805(13)	P(2)−C(31)	1.81(2)
P(2)−C(41)	1.82(2)		
P(1)−Au(1)−S	175.98(14)	P(1)−Au(1)−Au(2)	124.47(10)
S−Au(1)−Au(2)	51.97(9)	P(2)−Au(2)−S	171.72(12)
P(2)−Au(2)−Au(1)	120.84(9)	S−Au(2)−Au(1)	51.67(8)
C(71)−Au(3)−C(81)	93.1(5)	C(71)−Au(3)−C(91)	87.1(5)
C(81)−Au(3)−C(91)	179.5(4)	C(71)−Au(3)−S	176.0(3)
C(81)−Au(3)−S	87.2(4)	C(91)−Au(3)−S	92.6(4)
Au(1)−S−Au(2)	76.36(10)	Au(1)−S−Au(3)	92.64(12)
Au(2)−S−Au(3)	105.69(14)	C(11)−P(1)−C(51)	107.2(6)
C(11)−P(1)−C(61)	105.0(6)	C(51)−P(1)−C(61)	104.6(6)
C(11)−P(1)−Au(1)	111.0(5)	C(51)−P(1)−Au(1)	116.1(4)
C(61)−P(1)−Au(1)	112.1(4)	C(21)−P(2)−C(31)	106.1(6)
C(21)−P(2)−C(41)	107.8(6)	C(31)−P(2)−C(41)	105.0(7)
C(21)−P(2)−Au(2)	110.2(5)	C(31)−P(2)−Au(2)	114.8(5)
C(41)−P(2)−Au(2)	112.5(4)		

Au angles are also dissimilar. Of necessity, narrower Au−S−Au angles are correlated with shorter gold−gold contacts, and thus the narrower angle corresponds to that between the two gold(I) atoms, Au(1)−S−Au(2) = 76.36(10)°, whereas the angles between the gold(I) and gold(III) atoms are 92.64(12) and 105.69(14)°. The Au−S bond lengths to the gold(I) atoms, 2.332(3) and 2.342(4) Å, are longer than that in the starting material (2.300(2) Å)[20] and slightly shorter than those in the tetranuclear species $[S(Au_2dppf)\{Au(C_6F_5)_3\}_2]$[21] (2.339(3) and 2.343(3) Å); the Au−S distance to the gold(III) center is 2.374(4) Å, again shorter than in the tetranuclear complex (2.385(3) and 2.380(3) Å). The gold(I) atoms have a linear geometry with angles of 175.98(14) and 171.72(12)°; the gold(III) center has a square-planar geometry with *cis* angles that range from 87.1(5) to 93.1(5)°.

We have synthesized another mixed-valence gold derivative with a μ_3-sulfido unit in order to study these gold(I)−gold(III) interactions. The treatment of 2 equiv of $[S(Au_2dppf)]$ with $[Au(C_6F_5)_2(OEt_2)_2](OTf)$ (OTf = trifluoromethanesulfonate) affords a mixture of complexes from which it is possible to obtain the complex $[\{S(Au_2dppf)\}_2\{Au(C_6F_5)_2\}]OTf$ (**2**) as orange crystals. Complex **2** has only been characterized by means of X-ray crystallography. The cation of **2** is shown in Figure 3 and selected bond lengths and angles in Table 3. There are several gold−gold interactions (Figure 4); the shortest are those for gold(I)−gold(I) in the $[S(Au_2dppf)]$ units (2.9158(9) and 2.9511(9) Å). There is also a further gold(I)−gold(I) contact of 3.0436(8) Å between two gold atoms of different $[S(Au_2dppf)]$ units. However, the most significant features of this structure are the gold(I)−gold(III) interactions of 3.2195(8) and 3.3661(10) Å, the shorter being comparable to the gold(I)−gold(I) interactions in many molecules. The other gold(I)−gold(III) distances are longer, 3.786(1) and 3.799(1) Å. It is worthwhile pointing out the similarity between the structures of complexes **1** and **2**; both involve a μ_3-sulfido ligand bonded to two gold(I) atoms and one gold(III) atom, and the contacts are always between the two gold(I) centers and between one gold(I) and the gold(III) centers, without any further contact between the gold(III) and the other gold(I) atom. Again the narrowest Au−S−Au angles correspond to the shortest Au−Au distances, 76.89(11) and 78.20(11)° for the gold(I) atoms of the $[S(Au_2dppf)]$ units and 86.04(12) and 90.32(14)° for the shortest gold(I)−gold(III) interactions. The other Au−S−Au angles are 105.7(2) and 107.11(14)°, which are much wider than those mentioned above. For the gold(III) center, the coordination is planar with a mean deviation of 0.043 Å for the five atoms Au, 2 S, and 2 C. The Au(I)−S bond lengths lie in the range 2.319(4)−2.368(4) Å and the Au(III)−S in the range 2.387(4)−2.397(4) Å, values that are similar to those found in complex **1**.

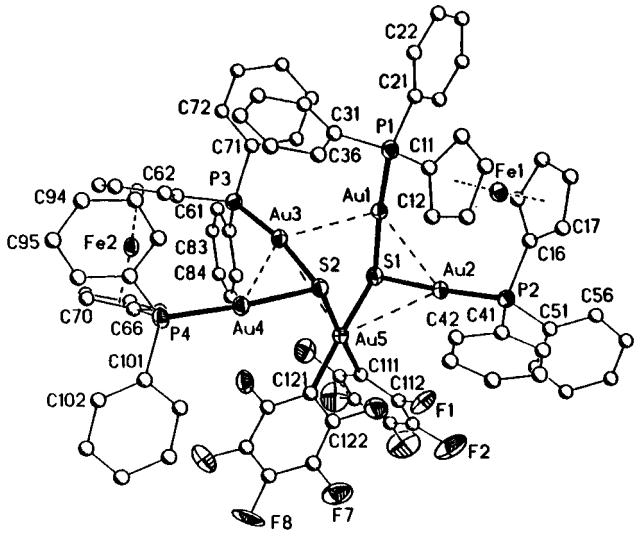

Figure 3. Perspective view of the cation of complex **2**. Displacement parameter ellipsoids represent 50% probability surfaces. Carbon atoms are spheres of arbitrary radius. H atoms are omitted for clarity.

Table 3. Selected Bond Lengths (Å) and Angles (deg) for Complex 2

Au(1)−P(1)	2.266(4)	Au(1)−S(1)	2.368(4)
Au(1)−Au(2)	2.9158(9)	Au(1)−Au(3)	3.0436(8)
Au(2)−P(2)	2.243(4)	Au(2)−S(1)	2.321(4)
Au(2)−Au(5)	3.2195(8)	Au(3)−P(3)	2.252(4)
Au(3)−S(2)	2.360(4)	Au(3)−Au(4)	2.9511(9)
Au(3)−Au(5)	3.3661(10)	Au(4)−P(4)	2.258(4)
Au(4)−S(2)	2.319(4)	Au(5)−C(111)	2.053(14)
Au(5)−C(121)	2.062(14)	Au(5)−S(2)	2.387(4)
Au(5)−S(1)	2.397(4)		
P(1)−Au(1)−S(1)	173.20(14)	P(1)−Au(1)−Au(2)	122.78(10)
S(1)−Au(1)−Au(2)	50.83(9)	P(1)−Au(1)−Au(3)	104.31(10)
S(1)−Au(1)−Au(3)	78.19(9)	Au(2)−Au(1)−Au(3)	113.00(2)
P(2)−Au(2)−S(1)	175.62(14)	P(2)−Au(2)−Au(1)	123.39(10)
S(1)−Au(2)−Au(1)	52.27(10)	P(2)−Au(2)−Au(5)	133.77(10)
S(1)−Au(2)−Au(5)	47.97(9)	Au(1)−Au(2)−Au(5)	76.33(2)
P(3)−Au(3)−S(2)	170.70(13)	P(3)−Au(3)−Au(4)	121.13(10)
S(2)−Au(3)−Au(4)	50.29(9)	P(3)−Au(3)−Au(1)	115.57(10)
S(2)−Au(3)−Au(1)	73.40(9)	Au(4)−Au(3)−Au(1)	123.06(3)
P(3)−Au(3)−Au(5)	133.03(11)	S(2)−Au(3)−Au(5)	45.17(10)
Au(4)−Au(3)−Au(5)	73.32(2)	Au(1)−Au(3)−Au(5)	72.49(2)
P(4)−Au(4)−S(2)	174.55(13)	P(4)−Au(4)−Au(3)	123.05(10)
S(2)−Au(4)−Au(3)	51.51(9)	C(111)−Au(5)−C(121)	88.6(5)
C(111)−Au(5)−S(2)	176.1(3)	C(121)−Au(5)−S(2)	91.1(4)
C(111)−Au(5)−S(1)	85.2(3)	C(121)−Au(5)−S(1)	173.7(4)
S(2)−Au(5)−S(1)	95.19(13)	C(111)−Au(5)−Au(2)	88.3(3)
C(121)−Au(5)−Au(2)	135.1(3)	S(2)−Au(5)−Au(2)	89.17(8)
S(1)−Au(5)−Au(2)	45.99(9)	C(111)−Au(5)−Au(3)	139.0(3)
C(121)−Au(5)−Au(3)	113.1(4)	S(2)−Au(5)−Au(3)	44.51(9)
S(1)−Au(5)−Au(3)	71.36(9)	Au(2)−Au(5)−Au(3)	97.97(2)

Molecular Orbital Calculations. The compounds described above present short Au−Au contacts between not only Au(I) atoms but also between Au(I) and Au(III) atoms. In order to understand their origin, we carried

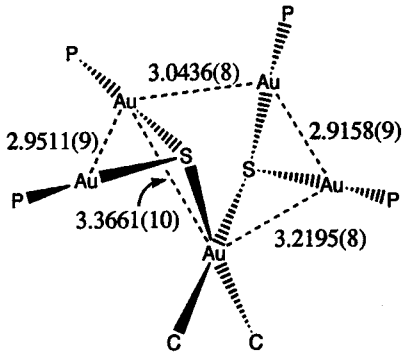

Figure 4. Main gold−gold contacts in complex **2**.

Chart 1

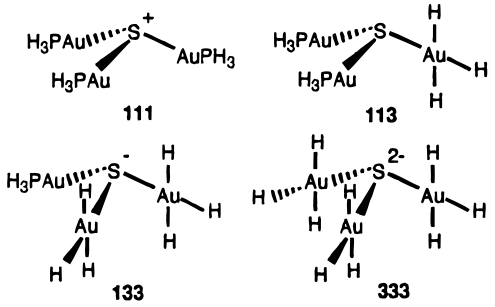

out density functional theory (DFT) and extended Hückel (EH) calculations on suitable model compounds.

In complex **1**, the two Au(I) centers are separated by only 2.8889(8) Å but are bridged by a ferrocenyl phosphine, whose bite may be determining in defining this distance. The relatively short Au(I)−Au(III) contact, on the other hand, is 3.404(4) Å, which is not such a short distance but is significantly shorter that the third one. Similar short distances are observed in compound **2**, those involving the Au(III) center being 3.3661 and 3.2195 Å, clearly longer than the 2.9158−3.0436 Å observed for Au(I) atoms.

To separate the effect of the bridging phosphine and also to minimize the size of the calculations, we used in our models the monodentate PH_3. The bulky ligands around Au(III) were replaced by H to have only a measure of electronic effects. In the DFT calculations, bulkier ligands could not be used in any event, owing to the size of the problem, but EH allows us to calculate the full molecule and therefore a comparison with the models can be attempted.

The problem to address is whether there are Au(I)−Au(III) interactions and, if there are, how they compare with Au(I)−Au(I). While the new gold compounds described in this work contain S bound to two Au(I) atoms and one Au(III) atom, other possible combinations are known, namely S bound to one Au(I) atom and two Au(III) atoms.[26] For this reason, a collection of four models was assembled; three were based on well-known structures of each type, namely $[S(AuPH_3)_3]^+$, (**111**), $[S(AuPH_3)_2(AuH_3)]$ (**113**), and $[S(AuPH_3)(AuH_3)_2]^-$ (**133**), and we decided to calculate also the unknown $[S(AuH_3)_3]^{2-}$ (**333**) (Chart 1). These correspond respectively to complexes containing Au(I)−Au(I)−Au(I), Au(I)−Au(I)−Au(III), Au(I)−Au(III)−Au(III), and Au(III)−Au(III)−Au(III).

(26) Chung, S.-C.; Krüger, S.; Schmidbaur, H.; Rösch, N. *Inorg. Chem.* **1996**, *35*, 4387.

Table 4. Results of the Geometry Optimization of and Comparison with Experimental Data and Related Calculations for $[S(AuPH_3)_3]^+$

distance/angles	ADF (NLA, R)	exptl	ref 17
S−Au (Å)	2.379	2.347, 2.301, 2.332	2.32 (fixed)
Au−Au (Å)	3.838	3.0187, 3.070	3.05
Au−S−Au (deg)	107.5	89.21, 80.99, 82.01	82.3

The DFT calculations were pursued in order to understand the structural preferences of the gold compounds, namely the sulfur environment. First, the geometry of $[S(AuPH_3)_3]^+$ was optimized under several conditions, using different possible basis sets and finally also nonlocal corrections. Only the introduction of the scalar relativistic approach led to the expected nonplanar structure, comparable to that found in the characterized compounds.[19] This system has also been addressed theoretically by Pyykkö *et al*, who found a preference for a pyramidal environment around sulfur, when their MP2 calculations included correlation and relativistic effects.[17]

Since $[S(AuPPh_2Me)_3]^+$ exhibits slightly different Au−Au distances, the structure of the model was partially optimized with only C_s rather than C_{3v} symmetry. The PH_3 ligand and the P−Au distance were kept fixed, while S−Au distances and Au−S−Au and S−Au−P angles were allowed to change. The final geometry showed no tendency to depart from C_{3v} symmetry, as expected. The geometric results of the final geometry optimization (distances in Å, angles in deg) are given in Table 4, along with experimental data and those calculated by Pyykkö *et al*.

Our calculations, when correlation and relativistic effects are taken into account, predict the molecule to be pyramidal, but on the other hand, the values for the distances and angles show a significant deviation from the experimental data. The MP2 calculations reproduce the experimental Au−S−Au angles, but they cannot be directly compared with ours, because the authors kept the Au−S distance fixed to the experimental value.[17] Even if their calculations also tended to elongate the Au−S bond, it would not be seen in the final results, as only angles are allowed to change and all distances are kept fixed. Therefore, on a qualitative level, our DFT calculations appear to give us the correct trend. The related oxygen derivatives $[O(AuPH_3)_3]^+$ have been studied as well using another DFT code (Gaussian 92),[26] and the calculated Au−Au distances are found to be too small (2.88 Å), while the related Au−O−Au angles are too low. The agreement between experimental and calculated values is again far from perfect, but as both the code and the system are different from ours, it is difficult to trace the origin of the disparity. Nevertheless, in both the oxygen and the sulfur compounds, there is a dimerization, which is most likely the reason lying behind the breaking of the C_{3v} symmetry. The intermolecular Au−Au distance is 3.0774 Å, comparable to the intramolecular ones. We made no attempt to model and study the dimeric species. Our approach appears to be reliable to get the qualitative trends of the geometry: the pyramidalization.

Some other mixed-valence Au complexes have been experimentally characterized. For our Au(I)−Au(I)−Au(III) model, we used $[S\{Au(PH_3)\}_2(AuH_3)]$, based on $[S(Au_2dppf)\{Au(C_6F_5)_3\}]$, (**1**). This model was partially

Table 5. Charges on the Gold Atoms of the Four Model Compounds

atom	Au(I)−Au(I)−Au(I)	Au(I)−Au(I)−Au(III)	Au(I)−Au(III)−Au(III)	Au(III)−Au(III)−Au(III)
Au(I)	1.29	1.25	1.28	
Au(III)		1.84	1.84	1.92

optimized as for the previous one, with C_s, though the real complex does not exhibit this symmetry, as one Au(I)−Au(III) distance is much shorter than the other (3.404 *vs* 3.758 Å). The Au−H distance is also allowed to change, but not the square-planar Au(III) environment and its orientation relative to the $Au^{I}SAu^{I}$ group. The final geometry shows a pyramidal environment for the sulfur atom, with shorter S−Au(I) (2.37 Å) than S−Au(III) bonds (2.57 Å). This result does not parallel the observed distances, respectively 2.332 and 2.342 Å for S−Au(I) and 2.374 Å for S−Au(III), where the difference is too small to be significant. The Au−Au distances are 3.54 Å between the two Au(I) atoms and 3.96 Å between Au(I) and Au(III), again much longer than 2.8889 Å or 3.404 and 3.758 Å. It may be added, though, that in this particular compound the two Au(I) centers are bridged by a ferrocenyl phosphine which may determine their distance, as it is much shorter than the normal Au(I)−Au(I) distance, as seen in the previous system we addressed (close to 3 Å). The S−Au−P angles are 177.38°, a bit larger than the 175.98, 171.72° found.

In conclusion, the calculations reproduce the pyramidality around the sulfur atom and indicate that the distance between the two Au(I) centers is significantly smaller than that between Au(I) and Au(III).

The next model, for Au(I)−Au(III)−Au(III), is the $[S\{Au(PH_3)\}(AuH_3)_2]^-$ anion, modeled after $[S\{Au(C_6F_5)_3\}_2(AuPPh_3)]^-$,[27] following the same lines as described above for the optimization procedure. The trends found in $[S\{Au(PH_3)\}_2(AuH_3)]$ are observed again. The S−Au(I) distance is only 2.342 Å, shorter than 2.618 Å for S−Au(III), both to be compared with 2.302 and 2.374 Å and 2.375 Å, respectively, in the real structure. The Au(I)−Au(III) distance is 3.773 Å, while Au(III)−Au(III) is 4.714 Å (the model has C_s symmetry), and in $[S(AuPPh_3)\{Au(C_6F_5)_3\}]_2^-$ they are all very similar (3.8997, 3.7694, 3.8516 Å). The Au(I)−Au(III) distances are comparable, but that is probably a coincidence. Accordingly, we cannot expect that the Au−S−Au angles in the model and the real molecule are very similar. It should be noticed, however, that there is some extent of pyramidalization around sulfur, as reflected by the Au−S−Au angles of 113.0, 107.4, and 108.4° (98.8 and 128.4° in the model). Another factor contributing to the disparity of results is certainly the bulk of the Au(III) ligands, which is not accounted for by the hydride ligand. The S−Au−P arrangement is almost linear (178.88°).

We come finally to our last model, Au(III)−Au(III)−Au(III), for which there is no experimental prototype. The molecule was optimized under C_s symmetry, and the results reflect this imposed symmetry. The S−Au bonds are 2.52 Å, which we may assume would be shorter in a real molecule, while the Au−Au distances are 4.14 and 4.04 Å. $[S(AuH_3)_3]^{2-}$ also shows a slightly pyramidalized sulfur atom, with angles Au−S−Au of 106.9 and 110.5°. These values parallel the behavior found for the AuH_3 units in the mixed-valence compounds. The Au−H bonds are 1.65 Å, comparable to the same type of bond in the other gold compounds.

These DFT calculations are able to reproduce the structural trends found in the Au(I), Au(III) SAu_3 derivatives. Before proceeding, we would like to compare the charges in the Au atoms (Table 5). They are very characteristic of the formal oxidation state of the gold atom considered and do not vary significantly from one compound to the other.

Standard extended Hückel calculations never predict the pyramidalization around sulfur in these or other compounds, but on the other hand, if we study the first model containing only Au(I), we can see that approaching two of these gold atoms always leads to the development of a positive overlap population. Going from a planar $[S(AuPH_3)_3]^+$ species to a pyramidal one results in weakening the S−Au bonds while the Au−Au interaction develops. When the Au−Au distance becomes 3.0 Å, the overlap population is 0.023, though the energy has increased by ca. 1 eV and the S−Au overlap population has fallen from 0.571 to 0.492. The reasons lying behind the development of such interactions have been well-studied before for Au(I)−Au(I).[28] What interests us here is the possibility of detecting Au(I)−Au(III) interactions.

Extended Hückel calculations performed on pyramidal $[S\{Au(PH_3)\}_2(AuH_3)]$, the model for Au(I)−Au(I)−Au(III), show that when sulfur becomes pyramidal, interactions between adjacent gold atoms appear, the overlap populations being (OP's) 0.021 for Au(I)−Au(I) and 0.003 for Au(I)−Au(III), suggesting the possibility of a Au(I)−Au(III) interaction. Before analyzing this situation in more detail, let us first consider the other two models, in order to get some more insight about these interactions in different environments. For the Au(I)−Au(III)−Au(III) model, $[S\{Au(PH_3)\}(AuH_3)_2]^-$, the OP's (for distances of 3.0 Å) are respectively 0.009 and −0.057 for Au(I)−Au(III) and Au(III)−Au(III), respectively. The short Au···Au distance forces a large amount of pyramidalization, and steric effects become important, obscuring the other features. Approaching gold atoms in a planar geometry leads to a much larger OP (0.027) between Au(I) and Au(III), reinforcing the idea that Au(I)−Au(III) interactions may indeed exist. The fourth model contains only Au(III) atoms, and pyramidalization never leads to a positive OP.

A simple binuclear model consisting of a linear AuH_2^- fragment and a square-planar AuH_4^- fragment which approach to form a Au(I)−Au(III) bond was used to test the Au(I)−Au(III) interaction. When the two gold atoms are 3.0 Å apart, their OP is 0.045. The simplified interaction diagram in Figure 5 shows the origin of this weak bond between the two gold atoms. In the Au(I) fragment, AuH_2^-, the HOMO is an Au−H σ^* x^2 orbital, derived from $x^2 - y^2$, z^2, and s, followed by one Au−H σ orbital based on x, while the two LUMO's are the y and z Au orbitals. In the Au(III) fragment, AuH_4^-, the metal

(27) Canales, F.; Gimeno, M. C.; Laguna, A. Unpublished results.

(28) (a) Calhorda, M. J.; Veiros, L. F. *J. Organomet. Chem.* **1994**, *478*, 37. (b) Veiros, L. F.; Calhorda, M. J. *J. Organomet. Chem.* **1996**, *510*, 71.

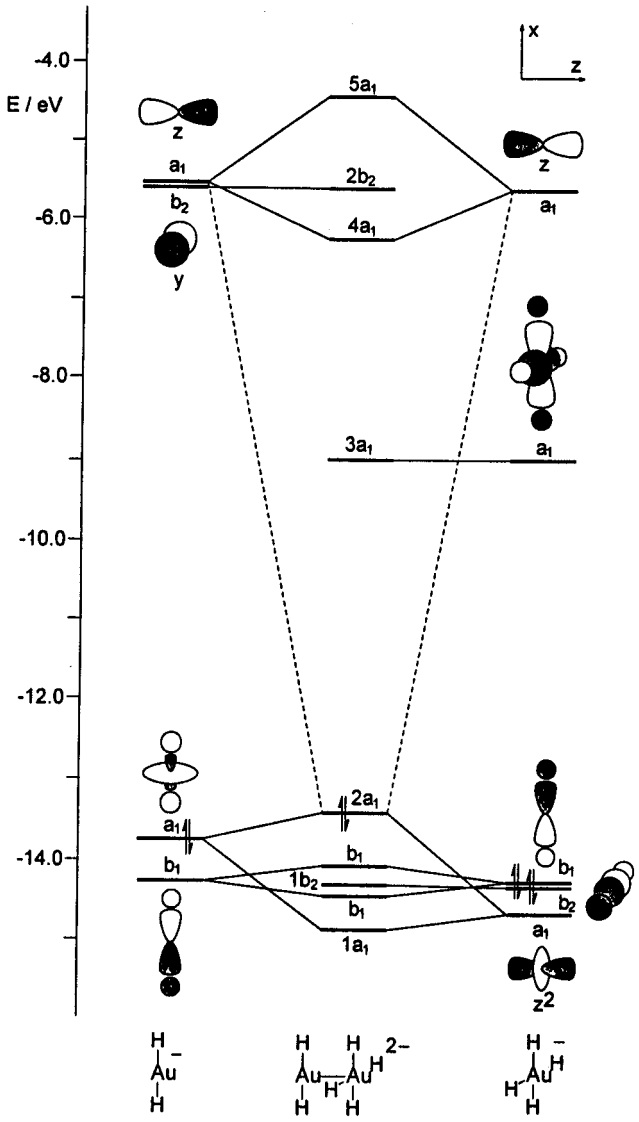

Figure 5. Interaction diagram between a d^{10} AuH_2^- fragment (left) and a d^8 AuH_4^- fragment (right).

is coordinated to more hydride ligands, so that the *y* orbital has also been pushed down to form another Au−H σ bonding MO. The LUMO of the Au(III) d^8 fragment, which is mainly $x^2 - y^2$, has been destabilized by the extra antibonding interactions with the hydride ligands.

The interaction between the two gold centers is clearly reminiscent of the interaction between two Au(I) centers, in that the main interactions involve occupied orbitals, although now one of them has a d^8 electronic configuration. The empty d orbital obviously cannot contribute to the formation of the Au−Au bond for symmetry reasons. Therefore, the HOMO of Au(I) interacts with the occupied orbital of the Au(III) fragment having the right symmetry, which is an essentially nonbonding z^2. As seen before for two Au(I) fragments,[28] the empty p orbitals oriented along the Au−Au axis mix in a bonding way into the resulting σ^* MO, making it less Au−Au antibonding, so that the global interaction becomes a bonding one. In the isoelectronic Au(I)−Pt(II)−Au(I), the HOMO also exhibits a metal-metal σ antibonding character, but its nature has not been discussed in detail.[29] It is then not surprising that some interaction similar to a Au(I)−Au(I) one can be found here. It should also be weaker, because the d orbital in Au(III) has a lower energy than that of Au(I) and mixing is less effective. The DFT calculations also indicated that the Au(I)−Au(III) distances are longer than Au(I)−Au(I) distances.

We can now analyze complex **1**, [S(Au_2dppf){Au(C_6F_5)$_3$}], containing Au(I)−Au(I)−Au(III). Extended Hückel calculations were performed using the experimental positions of the atoms in the structure and the OP value is 0.039 between Au1−Au2 (see Figure 2), the two Au(I) centers, separated by 2.9 Å; the distances between Au(I) and Au(III) are different, 3.4 and 3.8 Å, as the molecule is not symmetric, but the overlap populations are negative (−0.006, −0.009). This is not surprising, as these distances are extremely long compared to the 3.0 Å used in the calculations above and this is the most unfavorable geometry for Au(I)−Au(III) interactions.

Complex **2**, [{S(Au_2dppf)}$_2${Au(C_6F_5)$_2$}]OTf (Figure 3), can be seen as a kind of dimer of **1**, sharing the Au(III) atom. There are a few short distances, Au(I)−Au(I) and Au(I)−Au(III), Au(III) being Au5. The overlap populations calculated are respectively 0.036 (Au1−Au2, 2.9158 Å), 0.029 (Au1−Au3, 3.0436 Å), 0.029 (Au3−Au4, 2.9511 Å), 0.002 (Au2−Au5, 3.2195 Å), and −0.006 (Au3−Au5, 3.3661 Å). We note that the Au(I)−Au(I) distances are shorter and the OP values are all positive, as usual for this type of weak interaction. Also, in [S($AuPPh_2Me$)$_3$]$^+$, the Au(I)−Au(I)−Au(I) prototype, the distances are relatively long and the OP's consequently small (3.070 Å, 0.016; 3.0187 Å, 0.020) or even negative for the longest (3.2534 Å, −0.0003). On the other hand, the results for the two short Au(I)−Au(III) contacts in complex **2** are conflicting, as one OP is positive and the other negative. The negative one appears for the pair of atoms separated by the longest distance, Au3−Au5, very similar to that found in complex **1**. The positive value corresponds to the shortest Au(I)−Au(III) contact observed in the collection of compounds discussed. Indeed, for the complex [S($AuPPh_3$){Au(C_6F_5)$_3$}$_2$]$^-$, the Au(I)−Au(III) distances are 3.7794 and 3.8997 Å and the OP's are all negative. Considering all these results, it appears that Au(I)−Au(III) weak interactions are possible, though we can only detect one. In all the other situations, such interactions are prevented by other factors. Even packing forces may be stronger than these interactions.

Conclusions

Two new gold compounds were prepared where relatively short Au(I)−Au(III) distances were observed. DFT and EH calculations showed that in all the tested compounds the bridging sulfur atom prefers to have a pyramidal environment and that although Au(I)−Au(III) distances are slightly longer than Au(I)−Au(I) distances, there are reasons to believe there may be a weak interaction between the two gold atoms.

Experimental Section

Instrumentation and Materials. IR spectra were recorded on a Perkin-Elmer 883 spectrophotometer, over the range 2000−200 cm^{-1}, using Nujol mulls between polyethylene sheets. ^{1}H, ^{19}F, and ^{31}P NMR spectra were recorded on a

(29) Carlson, T. F.; Fackler, J. P., Jr.; Staples, R. J.; Winpenny, R. E. P. *Inorg. Chem.* **1995**, *34*, 426.

Varian UNITY 300 spectrometer in $CDCl_3$ solutions; chemical shifts are quoted relative to $SiMe_4$ (^1H, external), $CFCl_3$ (^{19}F, external), and H_3PO_4 (^{31}P, external). C, H, and S analyses were performed with a Perkin-Elmer 240C microanalyzer. Conductivities were measured in *ca.* 5×10^{-4} mol dm^{-3} acetone solutions with a Philips 9509 conductimeter, and Λ_M is given in Ω^{-1} cm^2 mol^{-1}. Mass spectra were recorded on a VG Autospec using FAB techniques and nitrobenzyl alcohol as matrix. The starting materials [S(Au$_2$dppf)],[20] [Au(C_6F_5)$_2$(OEt$_2$)$_2$]ClO_4,[30] and [Au(C_6F_5)$_3$(OEt$_2$)][31] were prepared as described earlier.

Synthesis. [S(Au$_2$dppf){Au(C_6F_5)$_3$}] (1). To a solution of [S(Au$_2$dppf)] (0.098 g, 0.1 mmol) in dichloromethane (20 mL) was added [Au(C_6F_5)$_3$(OEt$_2$)] (0.077 g, 0.1 mmol), and the mixture was stirred for 5 min. The solvent was evaporated to ca. 5 mL, and addition of hexane (15 mL) gave a orange solid of **1**, which was separated by filtration. Yield: 85%. Anal. Calcd for $C_{52}H_{28}Au_3F_{15}FeP_2S$: C, 36.87; H, 1.53; S, 1.93. Found: C, 37.21; H, 1.68; S, 1.91. $\Lambda_M = 15\ \Omega^{-1}$ cm^2 mol^{-1}.

[{S(Au$_2$dppf)}$_2${Au(C_6F_5)$_2$}]OTf (2). To a diethyl ether (20 mL) solution of [Au(C_6F_5)$_2$(OEt$_2$)$_2$]OTf (0.1 mmol) was added [S(Au$_2$dppf)] (0.196 g, 0.2 mmol) in dichloromethane (20 mL), and the mixture was stirred for 5 min. The solvent was evaporated to ca. 5 mL, and addition of diethyl ether (15 mL) gave a orange solid. Crystals of complex **2** were obtained by slow diffusion of diethyl ether in a dichloromethane solution of the orange solid.

X-ray Structure Determinations. Crystals were mounted in inert oil on glass fibers. Data were collected using monochromated Mo Kα radiation ($\lambda = 0.710\ 73$ Å). A Siemens P4 diffractometer with an LT-2 low-temperature attachment was used (scan type ω). Cell constants were refined from setting angles of *ca.* 65 reflections in the 2θ range 5−25°. Absorption corrections were applied on the basis of Ψ scans (**2**) or with the program SHELXA[32] (**1**). Structures were solved by direct methods (**1**) or the heavy-atom method (**2**) and refined anisotropically on F^2 (program SHELXL-93)[33] for all atoms except carbon. Hydrogen atoms were included using a riding model. To improve refinement stability, a range of restraints to local ring symmetry were employed. Special refinement details for complex **2**: three dichloromethane sites were refined (one disordered), and the values for M, D_{exptl}, etc. correspond to this ideal composition. Two further regions of ill-defined residual electron density probably correspond to further solvent but were not refined. Other data are collected in Table 6.

Molecular Orbital Calculations. Density functional calculations[34] were carried out on models using the Amsterdam Density Functional (ADF) program[35] developed by Baerends and co-workers[36] using nonlocal exchange and correlation corrections.[37] The geometry optimization procedure was based on the method developed by Versluis and Ziegler.[38] The relativistic effects were treated by a quasi-relativistic method, where Darwin and mass−velocity terms are incorporated.[39] In the first calculation, without relativistic corrections, the atom electronic configurations were described by a double-ζ Slater-type orbital (STO) basis set for H 1s (hydrogen atoms of the phosphine ligands), P 3s and 3p, S 3s and 3p, and Au 6s and 6p; a triple-ζ STO basis set was used for H 1s (hydride ligands). In all the other calculations, a double-ζ STO augmented with a single-ζ polarization function was used for H 1s (hydrogen atoms of the phosphine ligands), and a triple-ζ STO, augmented with a 3d single-ζ polarization function, was used for S and P 3s and 3p. A frozen-core approximation was used to treat the core electrons of P, S, and Au.

All the extended Hückel calculations were done using the extended Hückel method[40] with modified H_{ij} values.[41] The basis set for the metal atoms consisted of ns, np, and $(n-1)$d orbitals. The s and p orbitals were described by single Slater-type wave functions, and the d orbitals were taken as contracted linear combinations of two Slater-type wave functions. Only s and p orbitals were considered for S and P. The parameters used for Au were as follows (H_{ii} (eV), ζ): 6s −10.92, 2.602; 6p −5.55, 2.584; 5d −15.07, 6.163, 2.794 (ζ_2), 0.6442 (C_1), 0.5356 (C_2). Standard parameters were used for other atoms.

The calculations were performed on model complexes with idealized geometries taken from the real structures quoted in the text. Two stages of models were used. The first corresponds to more complex models where the ligands' bulky substituents were replaced by hydrogen atoms but the donor atoms were maintained. The second type of model, corresponding to the simplest ones, were created by replacing the

Table 6. Details of Data Collection and Structure Refinement for Complexes 1 and 2

	1	**2**·3CH_2Cl_2
chem formula	$C_{52}H_{28}Au_3F_{15}FeP_2S$	$C_{84}H_{62}Au_5Cl_6F_{13}Fe_2O_3P_4S_3$
cryst habit	orange prism	orange tablet
cryst size/mm	0.30 × 0.30 × 0.30	0.60 × 0.30 × 0.20
cryst syst	monoclinic	monoclinic
space group	$P2_1/n$	$P2_1/n$
a/Å	17.876(2)	18.214(3)
b/Å	18.559(2)	22.444(3)
c/Å	17.896(2)	24.081(3)
β/deg	104.074(8)	105.611(12)
U /Å^3	5759.0(11)	9481(2)
Z	4	4
D_c /Mg m^{-3}	1.936	2.029
M_r	1678.49	2895.63
F(000)	3136	5456
T/°C	−100	−100
$2\theta_{max}$/deg	45	45
μ(Mo Kα)/mm^{-1}	8.04	8.38
transmissn coeff	0.31−0.56	0.51−0.92
no. of rflns measd	7893	12707
no. of unique rflns	7421	12260
R_{int}	0.041	0.041
$R(F, F > 4\sigma(F))^a$	0.047	0.044
$R_w(F^2$, all rflns)^b	0.132	0.118
no. of params	407	525
no. of restraints	238	242
S^c	0.91	0.90
max $\Delta\rho$/e Å^{-3}	1.58	2.05

^{a} $R(F) = \sum||F_o| - |F_c||/\sum|F_o|$. ^{b} $R_w(F^2) = [\sum\{w(F_o^2 - F_c^2)^2\}/\sum\{w(F_o^2)^2\}]^{0.5}$; $w^{-1} = \sigma^2(F_o^2) + (aP)^2 + bP$, where $P = [F_o^2 + 2F_c^2]/3$ and a and b are constants adjusted by the program. ^{c} $S = [\sum\{w(F_o^2 - F_c^2)^2\}/(n-p)]^{0.5}$, where n is the number of data and p the number of parameters.

(30) Uson, R.; Laguna, A.; Arrese, M. L. *Synth. React. Inorg. Met. Org. Chem.* **1984**, *14*, 557.
(31) Uson, R.; Laguna, A.; Laguna, M.; Jiménez, J.; Durana, E. *Inorg. Chim. Acta* **1990**, *168*, 89.
(32) Sheldrick, G. M. SHELXA, a Program for Absorption Corrections. Unpublished report.
(33) Sheldrick, G. M. SHELXL-93, a Program for Crystal Structure refinement; University of Göttingen, Göttingen, Germany, 1993.
(34) Parr, R. G.; Yang, W. *Density Functional Theory of Atoms and Molecules*; Oxford University Press: New York, 1989.
(35) Amsterdam Density Functional (ADF) Program, release 2.01; Vrije Universiteit: Amsterdam, The Netherlands, 1995.
(36) (a) Baerends, E. J.; Ellis, D.; Ros, P. *Chem. Phys.* **1973**, *2*, 41. (b) Baerends, E. J.; Ros, P. *Int. J. Quantum Chem., Quantum Chem. Symp.* **1978**, *S12*, 169. (c) Boerrigter, P. M.; te Velde, G.; Baerends, E. J. *Int. J. Quantum Chem.* **1988**, *33*, 87. (d) te Velde, G.; Baerends, E. J. *J. Comput. Phys.* **1992**, *99*, 84.
(37) (a) Becke, A. D. *J. Chem. Phys.* **1987**, *88*, 1053; **1986**, *84*, 4524. (b) Vosko, S. H.; Wilk, L.; Nusair, M. *Can. J. Phys.* **1980**, *58*, 1200. (c) Perdew, J. P. *Phys. Rev.* **1986**, *B33*, 8822. (d) Perdew, J. P. *Phys. Rev.* **1986**, *B34*, 7406.
(38) (a) Versluis, L.; Ziegler, T. *J. Chem. Phys.* **1988**, *88*, 322. (b) Fan, L.; Ziegler, T. *J. Chem. Phys.* **1991**, *95*, 7401.
(39) (a) Ziegler, T.; Tschinke, V.; Baerends, E. J.; Snijders, J. G.; Ravenek, W. *J. Phys. Chem.* **1989**, *93*, 3050. (b) Snijders, J. G.; Baerends, E. J. *Mol. Phys.* **1978**, *36*, 1789. (c) Snijders, J. G.; Baerends, E. J.; Ros, P. *Mol. Phys.* **1979**, *38*, 1909.
(40) (a) Hoffmann, R. *J. Chem. Phys.* **1963**, *39*, 1397. (b) Hoffmann, R.; Lipscomb, W. N. *J. Chem. Phys.* **1962**, *36*, 2179.
(41) Ammeter, J. H.; Bürgi, H.-J.; Thibeault, J. C.; Hoffmann, R. *J. Am. Chem. Soc.* **1978**, *100*, 3686.

entire ligands with hydrogen atoms. The latter was used for the orbital analysis of the Au−Au interactions. These simplifications were tested and produced qualitatively similar results. The bond distances (Å) were as follows: Au−Au, 3.0; Au−P, 2.25; Au−S, 2.35; Au−H, 1.7; S−H, 1.3; P−H, 1.4.

Acknowledgment. We thank the Dirección General de Investigación Científica y Técnica (No. PB94-0079), the Fonds der Chemischen Industrie, the EU for HCM European network (Quantum Chemistry of Transition Metal Compounds, No. ERBCHRXCT 930156), and Acções Integradas Luso-Espanholas (Nos. E-56/96 and HP95-55) for financial support.

Supporting Information Available: Tables of crystal data, data collection, and solution and refinement parameters, bond distances and angles, positional parameters, and anisotropic thermal parameters for **1** and **2** (23 pages). Ordering information is given on any current masthead page.

OM970114S